Front. Phys. China, 2009, 4(2): 160–164
DOI 10.1007/s11467-009-0033-7

RESEARCH ARTICLE

Laser cooling and trapping of ytterbium atoms

Xin-ye XU (徐信业) (✉), **Wen-li WANG** (王文丽), **Qing-hong ZHOU** (周庆红), **Guo-hui LI** (李国辉), **Hai-ling JIANG** (蒋海灵), **Lin-fang CHEN** (陈林芳), **Jie YE** (叶捷), **Zhi-hong ZHOU** (周志红), **Yin CAI** (蔡寅), **Hai-yao TANG** (唐海瑶), **Min ZHOU** (周敏)

State Key Laboratory of Precision Spectroscopy and Department of Physics, East China Normal University, Shanghai 200062, China

E-mail: xyxu@phy.ecnu.edu.cn

Received February 23, 2009; accepted March 3, 2009

The experiments on the laser cooling and trapping of ytterbium atoms are reported, including the two-dimensional transversal cooling, longitudinal velocity Zeeman deceleration, and a magneto-optical trap with a broadband transition at a wavelength of 399 nm. The magnetic field distributions along the axis of a Zeeman slower were measured and in a good agreement with the calculated results. Cold ytterbium atoms were produced with a number of about 10^7 and a temperature of a few milli-Kelvin. In addition, using a 556-nm laser, the excitations of cold ytterbium atoms at $^1S_0$–$^3P_1$ transition were observed. The ytterbium atoms will be further cooled in a 556-nm magneto-optical trap and loaded into a three-dimensional optical lattice to make an ytterbium optical clock.

Keywords laser cooling and trapping, ytterbium, magneto–optical trap, optical frequency standards

PACS numbers 06.30.Ft, 32.80.Pj, 39.25.+k, 42.50.Vk

1 Introduction

With the help of laser cooling and trapping, especially the optical lattice technique, the optical atomic clocks with various atomic species developed in several institutes worldwide [1−4]. The alkaline-earth-metal atoms as well as the ytterbium atoms are promising candidates for optical frequency standards, owing to the existence of the milli-Hertz linewidth transitions between their singlet and triplet states [5, 6]. Recent experimental results show that the fractional frequency uncertainties of the strontium optical clocks are better than that of the cesium fountain atomic clocks [3, 7]. The optical frequency standards may become the next generation of frequency standards. Potentially, the optical frequency standards may help improve the accuracy and resolution of any present precision measurement results, such as the relative time variation of the fine-structure constant, the gravitational red shift, etc. However, the present measured clock instabilities are still two orders of magnitude away from the theoretical prediction, suggesting that we need to narrow further the linewidth of the probe laser and improve the signal-to-noise ratio. For the latter, it requires maximizing the signal or minimizing the noise. For this purpose, the experiments on the laser cooling and trapping of ytterbium atoms have been carried out for a while in several institutes around the world [4, 8−11].

Currently, we developed an apparatus for the laser cooling and trapping of ytterbium atoms to obtain a large number of cold atoms, expecting one order of magnitude better for the clock signal than the reported results. After the giant cold atoms are produced, they will be directly loaded into a three-dimensional optical lattice. Then we will use the ultra-narrow linewidth 578 nm laser to probe the clock transition. The observed ultra-narrow linewidth will be used for the frequency stabilization of the 578-nm laser, which will eventually provide an optical frequency standard.

2 Experimental setup

We used ytterbium atoms to develop an optical frequency standard. The whole system mainly consists of ultra-cold ytterbium atoms, a three-dimensional optical lattice, an ultra-narrow linewidth probe laser, and an optical frequency comb. In this article, we only focused on the experiments that produce cold ytterbium atoms.

Unfortunately, the vapor density of ytterbium atoms at room temperature is very low; usually, an ytterbium sample needs to be heated up to a temperature of a few hundred Celsius for vaporization. There are two methods to generate thermal ytterbium atoms for laser cooling experiments. One is heating an oven near the vacuum chamber, which was found to be not good for optical clock experiments due to blackbody radiation effects, and the other is using the Zeeman slowing technique, which was adapted in many laboratories due to not only providing a high-flux low-velocity atomic beam but also keeping the chamber at room temperature. We chose the latter to produce the thermal ytterbium atomic beam.

Generally, to obtain the ultra-cold ytterbium atoms, a two-stage cooling technique is employed, which includes broadband cooling and narrowband cooling. The relevant energy levels for laser cooling, an optical lattice, and a clock transition are shown in Fig. 1. It is well known that the capture velocity of the magneto-optical trap (MOT) is generally proportional to the linewidth of the transition used for cooling.

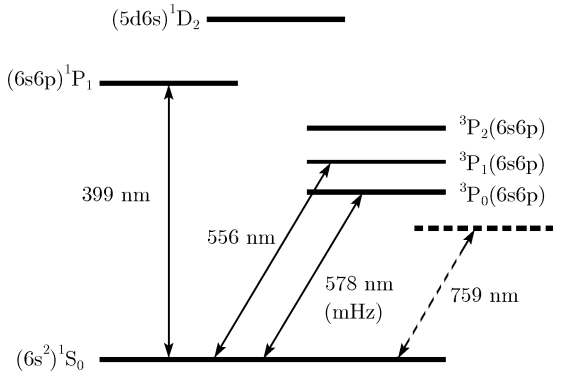

Fig. 1 Ytterbium atomic energy levels for the relevant cooling, trapping, and clock transitions.

Corresponding to the $^1S_0$–$^1P_1$ transition with a linewidth of 28 MHz, we estimated the capture velocity to be about 10 m/s. The velocities of the thermal atoms output from the Zeeman slower were about a few tens meters per second, suggesting that the $^1S_0$–$^1P_1$ transition is quite suitable for trapping and cooling ytterbium atoms in a MOT at the first stage; here, the wavelength of the corresponding cooling laser is 399 nm. On the other hand, according to the Doppler cooling theory, the Doppler-limited temperature of atoms after cooling is proportional to the transition linewidth, and the theoretically predicted temperature of ytterbium atoms cooled with the $^1S_0$–$^1P_1$ transition is about 0.7 mK, which is not low enough for the clock experiments, suggesting that further cooling process is necessary. Fortunately, the $^1S_0$–$^3P_1$ transition with a linewidth of 182 kHz is well adapted for this purpose due to the following reasons: the corresponding capture velocity is greater than the velocities of most atoms in the $^1S_0$–$^1P_1$ MOT, and the Doppler-limited temperature of atoms cooled with the $^1S_0$–$^3P_1$ transition is about 4 μK, which is very helpful for the efficient loading of atoms into the optical lattice. In addition, the linewidth of clock $^1S_0$–$^3P_0$ transition with a wavelength of 578 nm is about a few milli-Hertz. Eventually, we will use a 578-nm ultra-narrow linewidth laser to probe this clock transition precisely. The dashed line in Fig. 1 shows the virtual transition for the optical lattice with a wavelength of 759 nm.

The schematic diagram of the experimental setup for laser cooling ytterbium atoms is shown in Fig. 2, including an oven, a Zeeman slower, a collimating chamber with a pressure below 10^{-7} Pa, an interaction chamber with a pressure below 10^{-8} Pa, and the lasers with wavelengths of 399 nm (*solid lines*) for the first-stage cooling, 556 nm (*dashed lines*) for the second-stage cooling, 759 nm (*dashed and dotted lines*) for a three-dimensional optical lattice, and 578 nm (*thin solid lines*) for probing the clock transition.

Thermal ytterbium atoms were effused from an oven heated with a temperature of 773 K and went through two collimators with a separation of 12 cm and diameters of 3 and 6 mm, respectively. Entering the collimating chamber, the thermal atomic beam was further collimated by transversal cooling with the 399 nm laser light in two-dimensional optical molasses (2D-OM). Once the

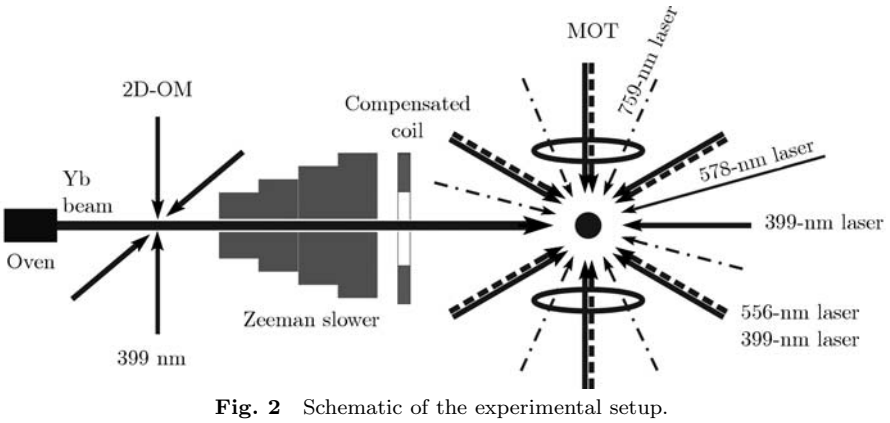

Fig. 2 Schematic of the experimental setup.

collimated atomic beam entered the Zeeman slowing region, where the magnetic field along the axis varied in distance, so that at any position the induced Zeeman shifts were exactly matched with Doppler shifts induced by the counter-propagating σ^- gaser beam, it was continuously decelerated. Finally, when the slowed atomic beam went into the MOT, the atoms were cooled and trapped by the six laser beams with a red detuning at a wavelength of 399 nm and the quadrupole magnetic field with a gradient of 5 mT/cm along the vertical direction at the center of the trap. Here, the 399 nm laser beams all came from the laser system, which was SYST TA–SHG 110 (Toptica Photonics), and were composed of an extended-cavity diode laser, a tapered amplifier, and a second harmonic generation. The output power of this laser system was about 120 mW at 399 nm. In addition, the compensated coil in Fig. 2 was used to compensate the magnetic field produced by the Zeeman slower at the MOT region. In this experiment, the laser beam output from second harmonic generation was split into two parts by a polarizing beam splitter. One was sent to the ytterbium MOT apparatus called as the main laser beam and the other was sent to the frequency locking system. The latter was first double-passed through an acousto–optic modulator, with a center frequency of 80 MHz and a bandwidth of 40 MHz for frequency tuning, and then sent to the frequency stabilization system where the modulation transfer spectroscopy was applied for frequency locking. The main laser beam was split into three beams by two polarizing beam splitters. The first beam was for 2D-OM called as the collimating beam, the second beam was for Zeeman slowing called as the Zeeman beam, and the third beam was for the MOT called as the MOT beam. The MOT beam was split into three beams by another two polarizing beam splitters, which again were sent into the interaction chamber along the three orthogonal directions. The Zeeman beam passed through a set of acousto–optic modulators and was frequency shifted to satisfy the Zeeman slowing condition. The collimating beam went through a set of lenses, so that it had a rectangle profile to interact with the ytterbium atomic beam along the propagation direction as long as possible.

3 Experimental results

There are many configurations of the Zeeman slower. We adapted a field-increasing configuration, suggesting that the magnitude of the magnetic field along the axis of the slower increased with distance; here, the distance is defined from the entrance of the slower as shown in Fig. 3.

We designed the slower with an effective length of 25 cm. For slowing the atoms from about 300 to 15 m/s within a distance of 25 cm, the required magnetic field distribution along the axis of the slower is shown in Fig. 3 as the dotted line. Based on the required distribution, we made a slower with the multilayer coils having a tapered shape. The measured and calculated magnetic field distributions are shown as dark dots and solid line in Fig. 3, respectively. We found that the measured, calculated, and required magnetic field distributions were in good agreement with each other.

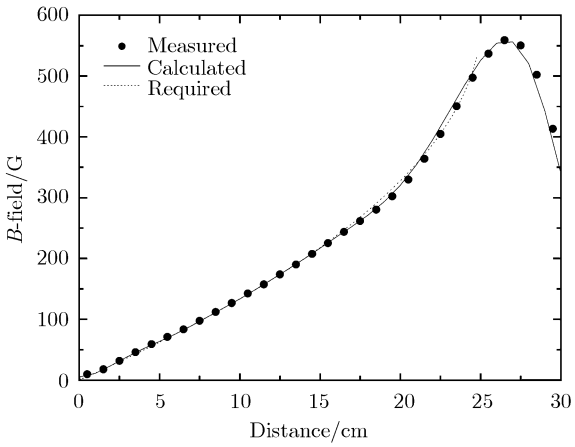

Fig. 3 Measured (*dark dots*), calculated (*solid line*), and required (*dotted line*) magnetic fields as functions of the distance along the axis of Zeeman slower.

The thermal atomic beam was first collimated in 2D-OM, then decelerated in the Zeeman slower, and finally flown into the 399-nm MOT to be trapped and cooled. Figure 4 shows an image of cold ^{174}Yb atoms in the MOT taken by a video camera. The power of each MOT laser beam was about 10 mW with a beam diameter of 25 mm, the power of the Zeeman laser beam was about 25 mW with a beam diameter of 10 mm, and the power of the collimating laser beam is about 30 mW with a beam size of 10 × 25 mm. We measured the loading and decay of the MOT at 399 nm by a photon detector through a lens system as shown in Fig. 5 where the signal-to-noise ratio was about 30. During the loading process, the thermal ytterbium atoms were captured and cooled by the 399-nm MOT from the slowed ytterbium atomic beam

Fig. 4 Image of cold ytterbium ^{174}Yb atoms in the 399-nm MOT.

continuously as shown in the left side of Fig. 5. After the 399-nm MOT has been on for 2 s, the B-field was turned off, and all laser beams were still kept on. Consequently, the cold atoms previously trapped in the MOT started to escape from the center of the MOT, so that the fluorescence signal decreased with time as shown in the right side of Fig. 5. The experimental data (*solid line*) were fitted very well by $y = y_0[1 - \mathrm{e}^{-t/(tl)}]$ for the loading process, where tl is the loading time, and $y = y_0 \cdot \mathrm{e}^{-t/(td)}$ for the decay process, where td is the decay time; all fitting curves were shown as dashed lines. We estimated the number and temperature of cold ^{174}Yb atoms in the 399-nm MOT to be about 10^7 (from the release-and-recapture measurement) and a few milli-Kelvin (from the time-of-flight measurements), respectively, at the first-stage cooling period.

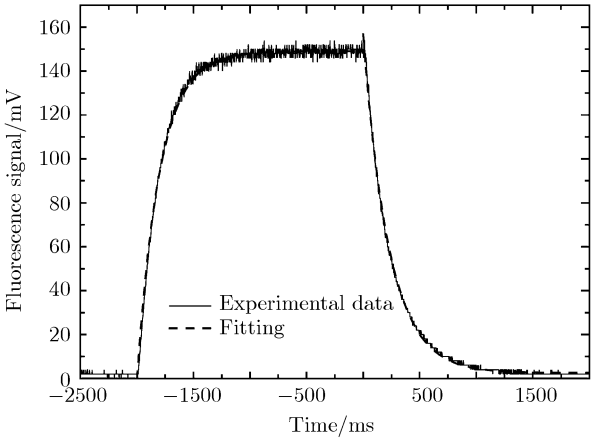

Fig. 5 Loading and decay curves in a 399 nm MOT. The experimental results are shown as filled circles, and the fitting results are shown as dashed lines.

We built the 556-nm laser system by direct frequency doubling of a fiber laser at 1111.6 nm with a periodically pooled MgO:$LiNbO_3$ waveguide. We sent the well-collimated laser beam with a power of 0.1 mW and a diameter of 2 mm into an additional ytterbium atomic beam apparatus, and the laser beam orthogonally interacted with the collimated ytterbium beam. The frequency of the 556-nm laser was scanned around the resonance frequency of the $^1S_0$–$^3P_1$ transition of the ^{174}Yb atoms. The fluorescence signal was collected by a photo-multiplier tube through a lens system. The photo-multiplier tube was located at a position that was perpendicular to the plane formed by the laser and atomic beams. The fluorescence signal as a function of the detuning of the 556-nm laser is shown in the bottom part of Fig. 6. On the other hand, we sent another 556-nm laser light with a power of about 10 mW into the interaction chamber interacting with the cold atoms in the 399-nm MOT. The laser beam was collimated with a diameter of 10 mm. The fluorescence signal of atoms in the 399-nm MOT was detected by a photon detector through a lens system. The top part in Fig. 6 shows the 399-nm fluorescence signal as a function of the detuning of 556 nm laser, which interacted with the cold atoms in the 399 nm MOT. Clearly, there was a peak corresponding to the resonance frequency of the $^1S_0$–$^3P_1$ transition, suggesting that cold ytterbium atoms were excited to $^3P_1$ and finally lost from the MOT. In other words, the 556-nm laser is ready for the second-stage cooling. Note that in Fig. 6 the ripples in the two sides of the top curve were induced by the 50 Hz noise, which we are now going to minimize.

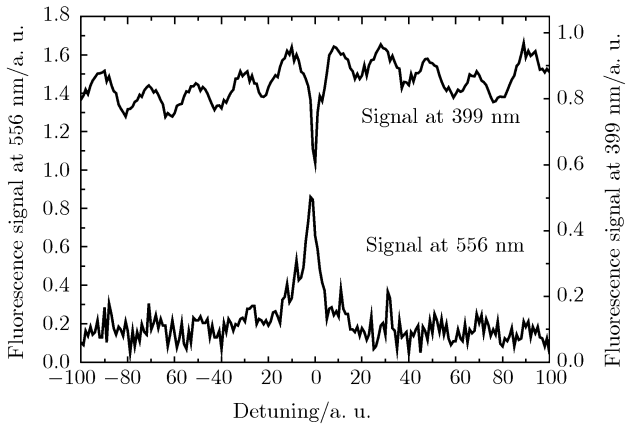

Fig. 6 Fluorescence signals of cold ytterbium atoms in the 399-nm $^1S_0$–$^1P_1$ MOT (*top curve*) and the ytterbium atomic beam (*bottom curve*) with respect to the detuning of the 556-nm laser relative to the resonance frequency of the 556-nm $^1S_0$–$^3P_1$ transition.

4 Conclusions

We studied the laser cooling and trapping of ^{174}Yb atoms in the 399-nm $^1S_0$–$^1P_1$ MOT. The cold atoms were excited at the $^1S_0$–$^3P_1$ transition by the 556-nm laser. We will further studr the second-stage cooling of ^{174}Yb atoms in the 556-nm $^1S_0$–$^3P_1$ MOT and load the ultra-cold atoms into the three-dimensional optical lattice. Finally, we will lock the frequency of an ultra-narrow laser at the $^1S_0$–$^3P_0$ transition of cold atoms in the optical lattice to obtain an ytterbium optical frequency standard, which could be applied in precision measurements and metrology.

Acknowledgements The authors are grateful to Long-sheng Ma and Zhi-yi Bi for helpful discussions. This work was supported by the National Natural Science Foundation of China (Grant No. 10774044), the National Key Basic Research and Development Program of China (Grant No. 2006CB921104), the Science and Technology Commission of Shanghai Municipality of China (Grant Nos. 06JC14026 and 07JC14019), and the Shanghai Pujiang Talent Program of China (Grant No. 07PJ14038).

References

1. M. Takamoto, F. Hong, R. Higashi, and H. Katori, Nature, 2005, 435: 321

2. A. Brusch, R. L. Targat, X. Baillard, M. Fouche, and P. Lemonde, Phys. Rev. Lett., 2006, 96: 103003
3. A. D. Ludlow, T. Zelevinsky, G. K. Campbell, S. Blatt, M. M. Boyd, M. H. G. de Miranda, M. J. Martin, J. W. Thomsen, S. M. Foreman, J. Ye, T. M. Fortier, J. E. Stalnaker, S. A. Diddams, Y. Le Coq, Z. W. Barber, N. Poli, N. D. Lemke, K. M. Beck, and C. W. Oates, Science, 2008, 319: 1805
4. N. Poli, Z. W. Barber, N. D. Lemke, C. W. Oates, L. S. Ma, J. E. Stalnaker, T. M. Fortier, S. A. Diddams, L. Hollberg, J. C. Bergquist, A. Brusch, S. Jefferts, T. Heavner, and T. Parker, Phys. Rev. A, 2008, 77: 050501(R)
5. Z. W. Barber, C. W. Hoyt, C. W. Oates, and L. Hollberg, A. V. Taichenachev, and V. I. Yudin, Phys. Rev. Lett., 2006, 96: 083002
6. Z. W. Barber, J. E. Stalnaker, N. D. Lemke, N. Poli, C. W. Oates, T. M. Fortier, S. A. Diddams, L. Hollberg, and C. W. Hoyt, A. V. Taichenachev, and V. I. Yudin, Phys. Rev. Lett., 2008, 100: 103002
7. T. P. Heavner, S. R. Jefferts, E. A. Donley, J. H. Shirley, and T. E. Parker, Metrologia, 2005, 42: 411
8. K. Honda, Y. Takahashi, T. Kuwamoto, M. Fujimoto, and K. Toyoda, Phys. Rev. A, 1999, 59: R934
9. T. Loftus, J. R. Bochinski, R. Shivitz, and T. W. Mossberg, Phys. Rev. A, 2000, 61: 051401(R)
10. C. Y. Park and T. H. Yoon, Phys. Rev. A, 2003, 68: 055401
11. R. Maruyama, R. H. Wynar, M. V. Romalis, A. Andalkar, M. D. Swallows, C. E. Pearson, and E. N. Fortson, Phys. Rev. A, 2003, 68: 011403